

# STUDY OF 2-IN-1 LARGE-APERTURE Nb<sub>3</sub>Sn IR QUADRUPOLES FOR THE LHC LUMINOSITY UPGRADE\*

V.V. Kashikhin, A.V. Zlobin<sup>#</sup>, FERMILAB, Batavia, IL 60510, U.S.A.

## Abstract

Double-aperture Nb<sub>3</sub>Sn quadrupoles with asymmetric coils and with cold and warm iron yokes were studied for the dipole-first upgrade scenario of the LHC Interaction Regions (IR). This paper describes the magnet design concepts and discusses their performance parameters, including field gradient and field quality limitations.

## INTRODUCTION

After operation at nominal parameters, LHC may be upgraded to higher luminosity. An interesting upgrade option includes the inner triplet with separation dipoles placed in front of the double-aperture focusing quadrupoles [1]. This option reduces the number of parasitic collisions and allows independent beam steering in the IR. However, the  $\beta_{max}$  in this layout is considerably larger for the same  $\beta^*$ . This requires using focusing quadrupoles with the largest possible aperture in 2-in-1 configuration with LHC beam spacing. Preliminary analysis based on the design study of single-bore Nb<sub>3</sub>Sn IR quadrupoles [2] showed that, for quadrupoles at the present nominal field gradient and critical current margin, the maximum aperture is limited by space considerations to 100 mm. Due to the close location of two high-gradient large-aperture quadrupoles in this magnet design, it is impossible to shield the coils from each other magnetically the way it is usually done in quadrupoles with larger beam separation to aperture ratio [3]. Thus, obtaining a reasonably good field quality in 2-in-1 magnet with 100 mm aperture may be challenging.

The goal of this work was to study possible field and field quality (dynamic aperture) limitations of 2-in-1 IR quadrupoles with the 100 mm bore, which can provide a nominal gradient of 205 T/m with 20% margin, and which are compatible with the horizontal LHC beam alignment and separation distance of 194 mm.

## MAGNET DESIGNS

The magnets have to provide opposite (focusing-defocusing) polarity for two counter-rotating beams as in the current LHC IR optics. Two different design concepts were considered: one with remote “warm” iron yoke and another one with closer “cold” iron yoke. Both designs were based on four-layer coils with the same Nb<sub>3</sub>Sn cables graded in the two outermost layers [2]. The cable parameters used in this study are summarized in Table 1.

### Warm yoke design

In the warm yoke design, the coils were placed inside a relatively thin common cylindrical iron yoke remote enough from coils to minimize the iron saturation effect

on field quality. The magnetic coupling between the coils and the yoke asymmetry with respect to each coil require the appropriate asymmetry in the coil geometry to obtain a good geometrical field quality.

First, the coil geometry was analytically optimized by ROXIE code [4] using a constant permeability ( $\mu=1000$ ) and a fixed inner radius of iron yoke to achieve a good geometrical field quality. Then the yoke outer radius was minimized using the ROXIE BEM-FEM solver while keeping the yoke saturation effect at an acceptable level. The yoke magnetic properties were described by B-H curve of low-carbon steel.

Fig. 1 shows the cross-section of optimized quadrupole coil inside the warm yoke with the inner radius of 315 mm and the outer radius of 400 mm. The cross-section has a different number of turns in the inner (49) and outer (61) quadrant coils.

In order to keep the saturation effect at an acceptable level in the operation field range, the yoke inner radius was chosen to provide the minimal distance from the coils of 125 mm. This space is sufficient for the coil support structure and cryostat components including thermal shield, cold-mass supports and vacuum vessel. The warm yoke approach results in a compact magnet design.

### Cold yoke design

In the cold yoke design, the iron yoke was placed closer to the coils. Due to a complicated yoke shape required in this case, there was no analytical solution available at low fields. Unlike the warm yoke design, the coil and yoke cross-sections were simultaneously optimized for a good geometrical field quality and low yoke saturation effect using the ROXIE BEM-FEM solver.

The optimized coil and yoke cross-sections for the cold yoke design are shown in Fig. 2. Due to the small distance between the coils, it was impossible to shield the coils magnetically from each other in this design too and the coils had to be asymmetric. However, the difference in the number of turns for the inner (53) and outer (62) quadrant coils necessary to obtain a good geometrical field quality is smaller than in the warm yoke design.

Table 1: Cable parameters.

Parameter	Unit	Layers	
		Inner	Outer
Number of strands		22	18
Strand diameter	mm	1.000	
Cable inner thickness (bare)	mm	1.656	1.679
Cable outer thickness (bare)	mm	1.910	1.886
Cable width (bare)	mm	11.183	9.138
Copper to non-copper ratio		1.2	
Insulation thickness	mm	0.18	

\*Work was supported by the US Department of Energy

<sup>#</sup>zlobin@fnal.gov

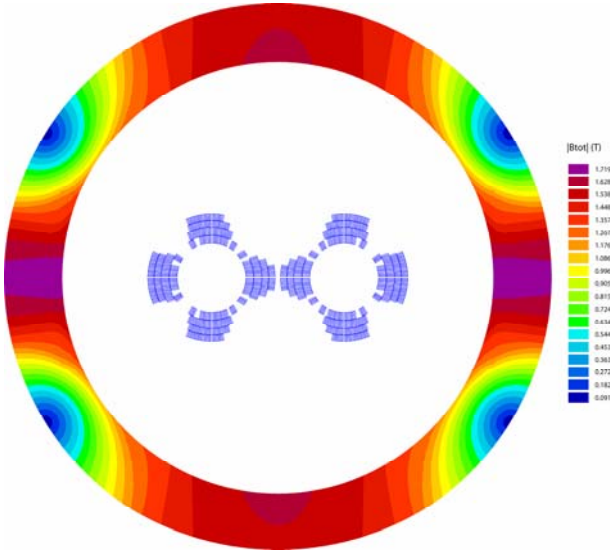


Figure 1: Coil and warm yoke cross-section with magnetic flux distribution in the yoke at 14 kA current.

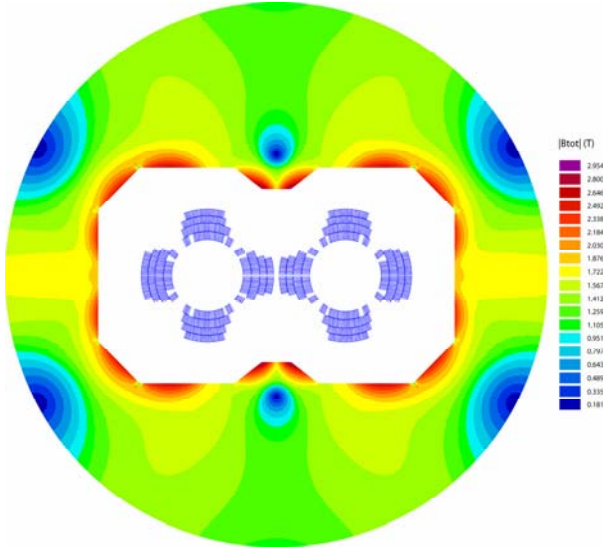


Figure 2: Coil and cold yoke cross-section with magnetic flux distribution in the yoke at 14 kA current.

## MAGNET PARAMETERS

Calculated parameters of the warm and cold yoke double-aperture quadrupoles are summarized in Table 2.

Table 2: Magnet parameters at  $T=1.9$  K and  $G=205$  T/m.

Parameter		Warm yoke	Cold yoke
Aperture diameter, mm		100	
Number of turns/aperture		220	230
Conductor area/aperture, cm <sup>2</sup>		72	75
Quench gradient, T/m		244	247
Quench current, kA		15.1	14.4
Peak field in the coil, T		14.1	14.3
Transfer function, T/m/kA		16.14	17.17
Inductance/aperture, mH/m		10.9	12.2
Stored energy/aperture, kJ/m		876	866
Lorentz forces/ 1 <sup>st</sup> octant	F <sub>x</sub> , MN/m	1.78	1.96
	F <sub>y</sub> , MN/m	-3.36	-3.21

The parameters responsible for magnet mechanical performance and quench protection for two designs are very close. In both cases, the target field gradient of 205 T/m with 20% margin can be achieved at a moderate critical current density in the coil of  $2500 \text{ A/mm}^2$  and quite large Cu/non-Cu ratio of 1.2:1.

Fig. 3 shows the quench gradient at 1.9 K as a function of the critical current density in the coil for both magnet designs. One can see that increasing conductor  $J_c$  from 2500 to  $3000 \text{ A/mm}^2$  increases the maximum field gradient in both designs by only 3%.

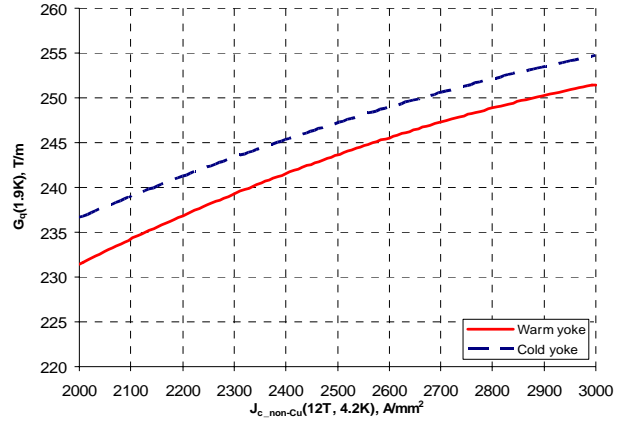


Figure 3: Quench gradient at 1.9 K.

Calculated field harmonics in the warm and cold yoke designs are reported in Table 3. Due to the coil and yoke asymmetry, the whole spectrum of normal harmonics is allowed in both designs. The low order harmonics were effectively suppressed using a wedge in each coil and midplane shims. The high-order harmonics are quite large in both designs. It was not possible to reduce them with additional wedges in the coil.

Table 3: Geometrical harmonics at 25 mm radius,  $10^{-4}$ .

Harmonic	Magnet design	
	Warm yoke	Cold yoke
$b_1$	0.0002	-0.0005
$b_3$	0.0001	0.0005
$b_4$	0.0001	0.0042
$b_5$	-0.0070	-0.0049
$b_6$	0.0014	-0.0305
$b_7$	0.0130	-0.0151
$b_8$	-0.0013	0.0996
$b_9$	-0.1016	0.0212
$b_{10}$	0.1797	0.3404
$b_{11}$	0.0799	0.1398
$b_{12}$	-0.0749	-0.0614
$b_{13}$	0.0447	0.0226
$b_{14}$	-0.0428	-0.0449

Fig. 4 shows the yoke saturation effect in the low order harmonics for the two designs. Variation of the dipole component in both designs was reduced to  $0.2 \cdot 10^{-4}$  units for the field gradients up to 205 T/m. Variations of the sextupole and higher order harmonics are negligibly small in the relevant gradient range.

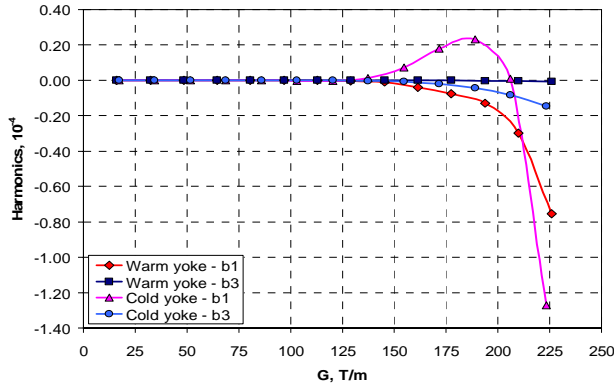


Figure 4: Yoke saturation effect.

## DYNAMIC APERTURE

Fig. 5 (a) shows the two round beams ( $9\sigma$ ) in Q2a/b at the nominal field gradient of 205 T/m in the present LHC inner triplet [5]. Analysis based on MQXB field quality measurements [6] shows that these two beams fit into the area (shown by the solid contour line) where deviations from the pure quadrupole field are less than  $10^{-4}$ . This area was considered as the dynamic aperture criterion of the nominal LHC IR. Note that in the above field analysis the harmonics that receive the active correction in LHC baseline IR optics ( $b_1$ ,  $b_3$ ,  $b_4$ ,  $b_6$  and  $a_1$ ,  $a_2$ ,  $a_3$ ,  $a_4$ ) were assumed to have zero values.

The area with the same  $10^{-4}$  deviations from the pure quadrupole field in both warm and cold yoke 2-in-1 quads, calculated using data presented in Table 3 and the baseline IR correction system, are shown in Fig 5 (b). For both 2-in-1 IR quadrupole designs, this area can accommodate the round beam of 54 mm in diameter. In spite of the relatively large high-order harmonics produced by the asymmetric coils, the dynamic aperture spans 54% of the physical aperture for the 2-in-1 designs which is only by 2% smaller than the ratio of the dynamic to physical aperture of the baseline IR quadrupoles. However, the calculations made for  $\beta^*=0.25$  m show that the necessary beam aperture is 54-64 mm (depending on the model used) [5], which is 0-18% larger than the dynamic aperture.

## CONCLUSION

The 2-in-1  $\text{Nb}_3\text{Sn}$  quadrupoles suitable for the dipole-first upgrade scenario of the LHC IR region have been studied. The maximum aperture for the LHC beam separation distance and nominal gradient is limited by the coil size at 100 mm. Two possible design approaches based on the warm and cold iron yokes were analyzed. It was shown that these designs have very similar operating parameters that allow making a design choice based on preferable mechanical or cryogenic system considerations. The dynamic aperture is practically the same for both designs and spans about the same fraction of the physical aperture as in the baseline  $\text{NbTi}$  IR quadrupoles. However, it may be the limiting factor for IR optics with  $\beta^*=0.25$  m.

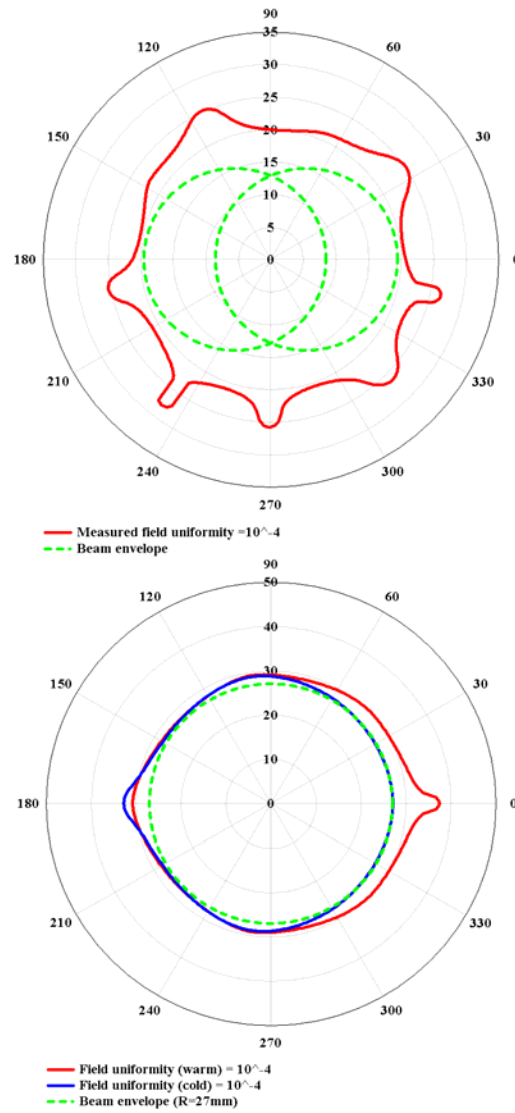


Figure 5: Dynamic apertures of the present single-aperture  $\text{NbTi}$  LHC IR quads (top) and 2-in-1  $\text{Nb}_3\text{Sn}$  quads (bottom).

## REFERENCES

- [1] J.B. Strait, et al., "Towards a New LHC Interaction Region Design for a Luminosity Upgrade", Proc. of 2003 Particle Accelerator Conference, Vol. 1, p. 42.
- [2] A.V. Zlobin, et al., "Aperture limitations for 2nd generation  $\text{Nb}_3\text{Sn}$  LHC IR quadrupoles", Proc. of 2003 Particle Accelerator Conference, Vol. 3, p.1975.
- [3] V.V. Kashikhin, A.V. Zlobin, " $\text{Nb}_3\text{Sn}$  Arc Quadrupole Magnets for VLHC", Proc. of 2001 Particle Accelerator Conference, Vol. 5, p. 3412.
- [4] S. Russenchuck, "A Computer Program for the Design of Superconducting Accelerator Magnets", CERN AT/95-39, LHC Note 354, Sept. 26, 1995.
- [5] [http://care-hhh.web.cern.ch/care-hhh/SuperLHC\\_IRoptics/IRoptics.html](http://care-hhh.web.cern.ch/care-hhh/SuperLHC_IRoptics/IRoptics.html)
- [6] G.V. Velez et al., "Field Quality Measurements of the LQXB Inner Triplet Quadrupoles for LHC", IEEE Trans. on Applied Superconductivity, Vol. 15, No. 2, June 2005, p. 1102.